Numerical simulation of air jet attachment to convex walls and application to UAV

Nikola Mirkov and Boško Rašuo

Abstract In this paper, we present a numerical study of the wall jet flow over a convex surface, viz. the Coanda wall jet, and its application to a conceptual Unmanned Aerial Vehicle (UAV) design which uses the Coanda effect as a basis of lift production. This configuration is important in a way that it considers the Coanda wall jet over a smooth convex wall with non-constant curvature, in contrast to most of the previous situations where only constant curvature walls were considered e.g. the Coanda wall jet over circular cylinder. To enable the mathematical representation of this complex geometrical configuration, we propose a form of a parametric representation of the conceptual geometry, based on Bernstein polynomials, which is universal in character and spans a complete design space. It is shown how dynamically changing the flow picture enables smooth change of net forces on the body. Capability to control the direction of the net force is shown to be useful for maneuvering the UAV. All simulations are done using an open-source finite-volume computational fluid dynamics code based on Reynolds-averaged Navier-Stokes equations. Turbulence is accounted for using the $k-\omega$ Shear Stress Transport model.

1 Introduction

Turbulent air jets have a natural tendency to attach to the walls when blown close to them. After the air jet is issued into the quiescent surrounding, it entrains the air between the jet and the wall. Low pressure region is formed causing the jet to deflect towards the wall. This phenomenon known as the Coanda-effect has found

Nikola Mirkov
University of Belgrade, Institute of Nuclear Sciences - Vinca, Mike Alasa 12-14, Belgrade, Serbia,
e-mail: nmirkov@vinca.rs

Boško Rašuo
University of Belgrade, Faculty of Mechanical Engineering, Kraljice Marije 16, Belgrade, Serbia,
e-mail: brasuo@mas.bg.ac.rs

diverse applications ever since it was discovered. Most applications came out of an observation that Coanda wall jet is an efficient way of generating aerodynamic force. Underneath the attached wall jet static wall pressure falls below the ambient pressure causing the aerodynamic force on the body.

Conceptual designs such as no tail rotor (NOTAR) helicopter, and aerodynamic devices like circulation control airfoils on vertical and short take-off and landing aircaft (V/STOL) are examples of successful application of Coanda wall jets. The use of Coanda wall jets as a primary mechanism for producing the lift force of the aircraft mostly remained in the blind spot of the aerodynamic community at least until the wider popularity of Unmanned Aerial Vehicles (UAV). Owing to the UAV, interest in the aircraft that produce lift with the aid of the Coanda-effect has been renewed in recent times. The need to address the aerodynamics of these aircraft in a systematic way has become present. The power available for the hover and maneuvering should be used as economically as possible. A need for thorough experimental and numerical tests is obvious.

Wygnanski and co-workers did an experimental study of the curved wall jets [1–5] observing that curved wall jet had greater spreading rate than the plane wall jet. They were observing large stream-wise vortices that increased turbulent momentum exchange which lead to faster spreading rates. In [6] more experimental evidence was given to support the view of wall curvature being responsible for maintenance the stream-wise coherent structures.

Numerical studies of the Coanda wall jets using direct numerical simulation (DNS), as well as large eddy simulation (LES) are scarce, mostly due to a large range of scales present in these flows. In [7, 8] DNS is used to simulate configuration from the experiments of Wygnanski and coworkers confirming their observations related to the appearance and role of stream-wise vortices. Numerical studies relying on Reynolds Averaged Navier-Stokes approach with linear eddy-viscosity models (LEVM) were employed in several cases, such as [9, 10]. Most of the difficulties faced when using LEVM resulted from neglecting the influence of curvature in derivation of these models. LEVM models led to under-prediction of wall jet spreading rate and over-prediction of skin friction coefficient.

All simulations in [9] showed great dependency on jet inflow conditions and transition process. Results from [9] indicated that Menter's $k-\omega$ SST model gave relatively good results when the wall pressure coefficient was predicted, which is significant for the present study. Because of the high computational cost of LES or DNS simulations for this type of flows, and because of our interest primarily in pressure distribution responsible for lift generation, we decide to use the SST model for our study interpreting the results cautiously, having in mind previous general criticism of LEVM models. Among other things, this paper is focused on conceptualizing the geometric shape of the aircraft which uses Coanda wall jet for lift production. Consequently, the Coanda wall jet studied in this paper differs from the previous ones since the wall jet is attached to a wall with no constant curvature, as postulated in other works [7–10] where wall jet attaches to the surface of the circular cylinder.

2 Definition of geometry

In this section, the geometry chosen for the current investigations and its parametric representation are described. The way geometry is represented strongly affects the optimization process. In [11–13], it is shown how different airfoils, axially symmetric bodies, and other more complex three dimensional shapes (wings, fuselages, etc.) can be represented by means of the class function, shape function representation, within the 'CST' approach. The class function is used to define a general class of geometries, while the shape function is used to define specific shapes within the geometry class.

The main idea presented in these papers is to decompose the basic shape into scalable elements corresponding to discrete components by representing the shape function with a Bernstein polynomial. The Bernstein polynomial of order n is composed of the $n+1$ terms of the form:

$$S_{r,n}(\psi) = K_{r,n}\psi^r(1-\psi)^{n-r}, \tag{1}$$

$$K_{r,n} \equiv \binom{n}{r} \equiv \frac{n!}{r!(n-r)!}, \tag{2}$$

where factors $K_{r,n}$ are binomial coefficients as shown above. Fig. 1 shows an example of unit function decomposition using Bernstein polynomials of sixth degree. By scaling any component in the unit function representation we can make well localized, small variations of that function. The geometry of cross section of a Coanda-

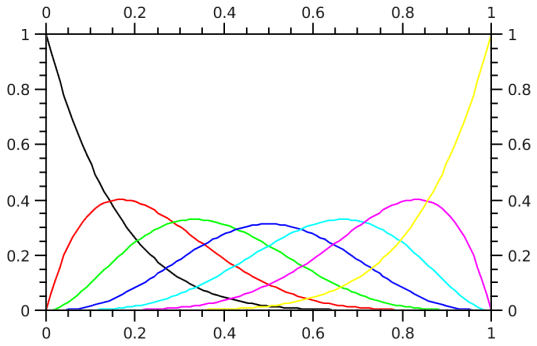

Fig. 1 The unit function decomposition using 6^{th} degree Bernstein polynomial.

effect UAV is similar to elliptic-arc. Therefore, the class function will be the function defining an elliptic arc,

$$\zeta(\psi) = A\psi^{0.5}(1-\psi)^{0.5}. \tag{3}$$

By adjusting the coefficient A in the class function representation, one can choose the aspect ratio of an elliptic arc. Taking A to be equal to two, gives a circle. By scaling the coefficients in the component representation of a shape function, we can

derive appropriate variations of the basic shape. Fig. 2a shows decomposition of an ellipse ($A = 0.7$) using Bernstein polynomials of sixth degree. We need to emphasize that the order of Bernstein polynomial, used for the function decomposition, is chosen freely. The higher order makes more localized variations of the basic shape possible. For our numerical studies, we used geometry defined by the following

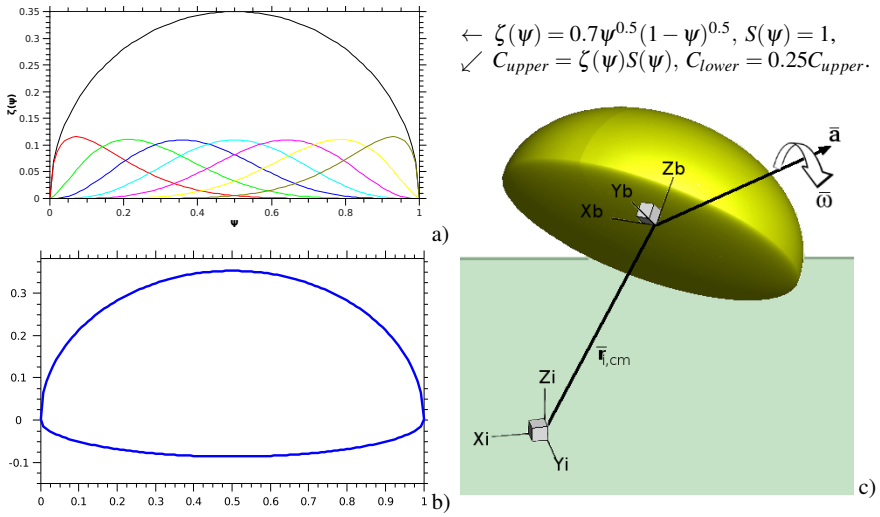

Fig. 2 Definition and universal parametric representation of the UAV shape: a) Bernstein polynomial decomposition of an elliptic arc $\zeta(\psi)$, b) Cross-section defined by C_{upper} and C_{lower}. c) 6-DOF motion of the Coanda effect UAV.

expressions. The upper contour is defined by

$$C_{upper}(\psi) = \zeta(\psi)S(\psi), \tag{4}$$

where

$$\zeta(\psi) = 0.7\psi^{0.5}(1-\psi)^{0.5}, \tag{5}$$

and

$$S(\psi) = 1. \tag{6}$$

The value of the parameter ψ lies in the interval $\psi \in [0,1]$. The lower contour is defined by

$$C_{lower}(\psi) = 0.25C_{upper}(\psi). \tag{7}$$

The final cross-section shape is shown in Fig. 2b, and an illustration of complex rigid body motions the UAV with Coanda effect-based lift production can undergo is shown in Fig. 2c. Using the 'CST' method, we are able to define various contour shapes by scaling the components of Bernstein polynomial representation of the unit shape function. This technique has the following properties:

- Present contour representation technique captures the entire design space of smooth geometries.
- Every contour in the entire design space can be derived from the unit shape function contour.
- Every contour in the design space is derivable from every other.

With this technique it is easy to construct various shapes of the UAV based on Coanda-effect and compare their performances.

3 Numerical method

Simulations are performed using the authors' own open-source code [14], implementing cell-centered, second-order accurate finite volume discretization of Reynolds-Averaged Navier-Stokes equations (RANS). The code is intended for block structured non-orthogonal geometries, with collocated variable arrangement. The pressure correction and momentum equations are solved iteratively using the SIMPLE algorithm [15]. The discretization schemes are second-order accurate. Turbulence is accounted using Menter's $k-\omega$ Shear-Stress Transport model. Automatic wall boundary condition approach [16] is used. It is particularly suited when, during geometric multigrid procedure, a wall-coarsening takes place, which requires a paradigm shift in treating the cells in the first layer next to the wall, because of the difference in y^+ values. O-type structured body-fitted meshes were generated with refined layers towards the wall. Aerodynamic forces acting on a body immersed in fluid are calculated in a usual way – pressure and viscous forces are integrated over the body surface to give net forces.

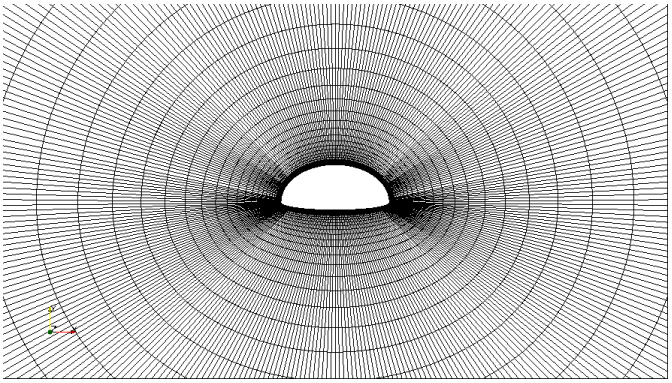

Fig. 3 Detail of the computational grid. Grid is successively refined toward the wall. Along the wall, mesh is piecewise uniform, with increased grid density in the region of high curvature. Grid density discontinuities are seen as 'rays' emanating from the body.

4 Simulation setup and results

The case that we have studied has moderately small Reynolds number, $Re = 63775$ based on mean velocity and inlet height. Velocity is uniform across the inlet ($U_b =$ 20 m/s). Such velocity distribution at inlet is chosen in accordance to [9] where a top-hat velocity profile is used at inlet. We have not considered any particular method by which the inlet flow is generated. We have to remind, however, that in such case some additional information should be provided, such as swirl velocity component, if a fan is used for providing inflowing air. To generate lateral forces which would produce forward motion, we experimented with varying inlet velocity along the circumference of the inlet, resulting in an asymmetric Coanda effect.

Single block O-type grid was used with roughly 50 000 cells. Three increasingly refined grids were used in geometric multigrid approach. Grid points are clustered toward to wall, and in the direction along the wall mesh is piecewise uniform, with increased grid density in the region of high wall curvature, i.e. where upper and lower aerodynamic surface meet, which is also, under such conditions, a region of wall jet separation. A detail of the mesh around the UAV body is shown in Fig. 3.

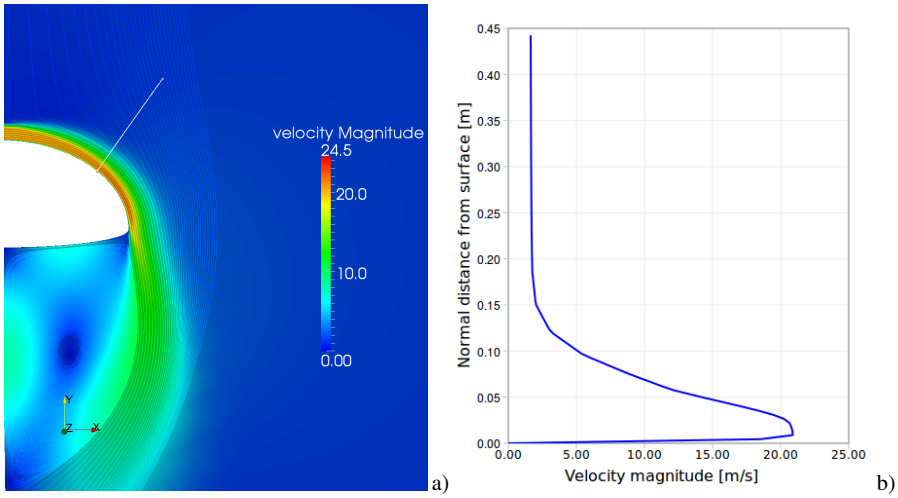

Fig. 4 Velocity magnitude profiles along surface normal at wall surface position defined by the point's radius vector angle with horizontal plane, $\theta = 30^\circ$.

In [17, 18] the symmetric configurations are studied to numerically estimate total lift force needed for hovering flight. In Fig's. 4-6 we show the development of velocity profile along the upper surface. The profiles are taken along surface normal, at positions defined by angle θ, which is the angle between the radius vector of the point at the body's surface and the horizontal plane. Distribution of the pressure coefficient over the body's surface is shown in Fig. 7.

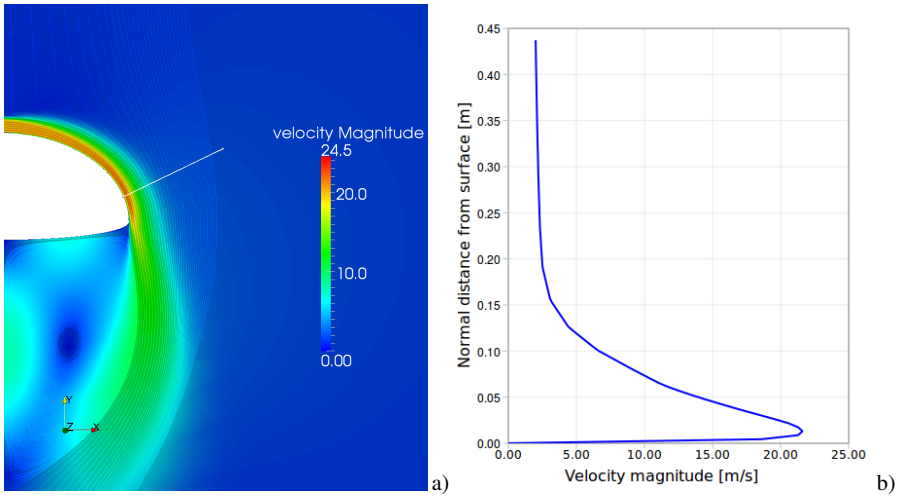

Fig. 5 Velocity magnitude profiles along surface normal at wall surface position defined by the point's radius vector angle with horizontal plane, $\theta = 10^{\circ}$.

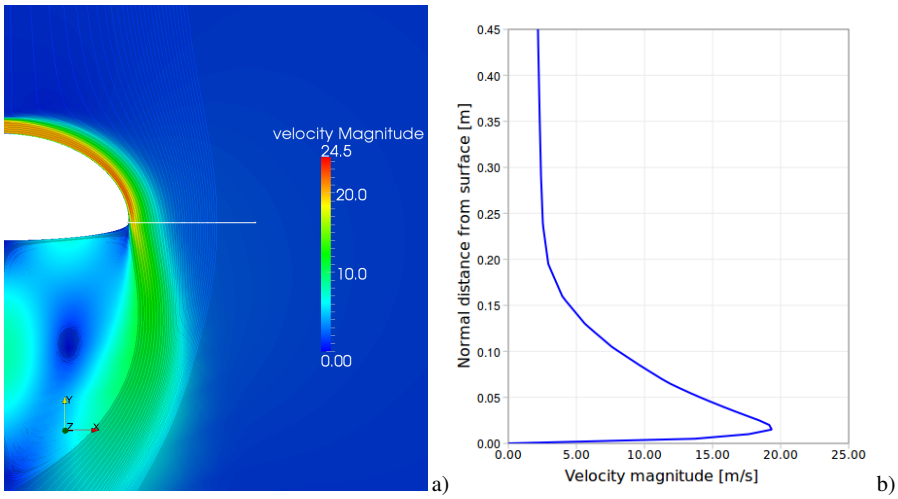

Fig. 6 Velocity magnitude profiles along surface normal at wall surface position defined by the point's radius vector angle with horizontal plane, $\theta = 0^{\circ}$.

Next, we focus on changes in aerodynamic forces, needed for aircraft maneuvering by varying the inlet conditions. The nozzle air-speed ratio, e.g. 20/15, determines the nozzle air-speeds in $[m/s]$ at opposite directions. In three-dimensional configurations nozzle air speed changes continuously along the circumference.

The streamlines and velocity contours are shown for the 20/15 case in Fig.8. Fig.9 shows the pressure coefficient distribution change for asymmetric flow conditions as the nozzle air-speed ratio is varied. Similar to symmetric situation, in all cases

the pressure coefficient has the lowest value at the upper surface edge, indicating maximum wall-jet velocity being reached there - a consequence of the Coanda effect. Finally, Fig. 10 shows the resulting pressure force components for asymmetric flow cases.

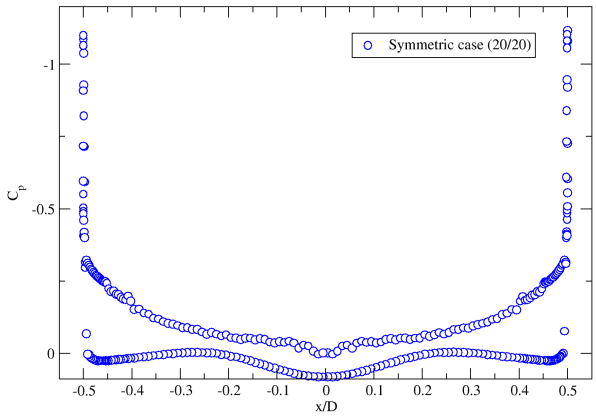

Fig. 7 Pressure coefficient distribution for symmetric conditions needed for hovering.

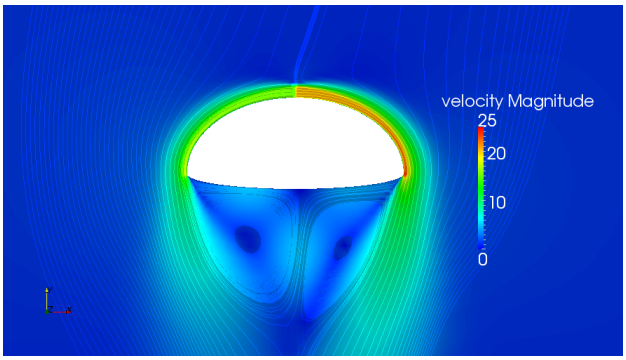

Fig. 8 Velocity contours and streamlines for 20/15 nozzle air-velocity ratio.

5 Discussion and conclusion

In this paper, we present the numerical study based on finite volume discretization algorithm of RANS equations closed by LEVM model of turbulent wall jet flow over convex surface with non constant curvature. The distinguished features of the flow are jet attachment to wall as a consequence of the Coanda effect, entrainment of surrounding air and jet spreading, massive separation in the region of high curvature, and formation of the large recirculation region. All these features combined make

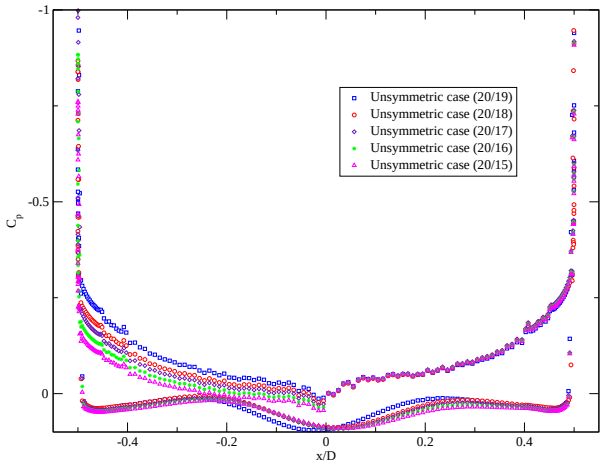

Fig. 9 Pressure coefficient distribution for various nozzle air-velocity ratios.

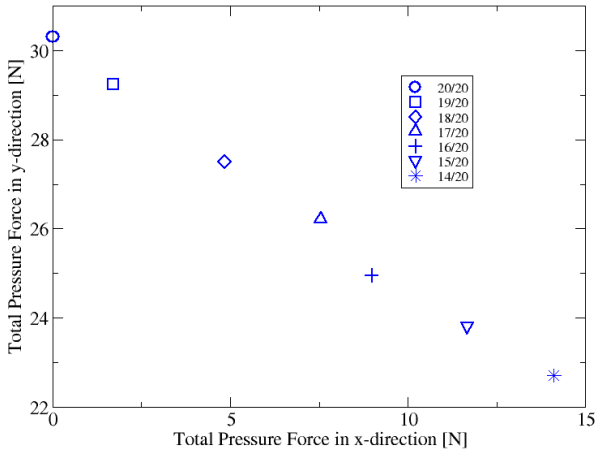

Fig. 10 Total pressure force for various nozzle air-velocity ratios.

this type of flow very difficult to simulate accurately. The motivation to do so comes from an interesting and very useful application to UAV.

Using numerical simulation we were able to tackle the fascinating and not fully exploited phenomena of the Coanda effect-based lift production. It is shown here that by gradually changing the flow picture around the UAV by varying jet inflow air-speed along the circumference of the revolving body, we change the resulting force in a smooth way. The UAV is tilted by asymmetric lift distribution under these conditions, the horizontal component of the resulting force appears, producing forward flight conditions. A small change in inlet velocity does not lead to great change in the resulting force, a favorable circumstance which indicates that maneuverabil-

ity of such a configuration is possible using this mechanism. Future investigations will deal with non-stationary simulation and coupling of fluid and 6-DOF solver to enable further insight into the characteristics of Coanda effect based UAV lift production, and investigate different mechanisms to achieve its efficient maneuverability.

Acknowledgements The authors gratefully acknowledge the financial support of Serbian Ministry of Education, Science and Technological Development for the financial support of this research trough projects TR-33036 and TR-35006.

References

1. Neuendorf, R., and Wygnanski, I.: On a Turbulent Wall Jet Flowing over a Circular Cylinder. J. of Fluid Mechanics, **381**, 1–25 (1999)
2. Neuendorf, R.: Turbulent Wall Jet Along a Convex Curved Surface. PhD Thesis, Univ. of Berlin, Berlin (2000)
3. Cullen, L.M., Han, G., Zhou, M.D., and Wygnanski, I.: On the Role of Longitudinal Vortices in Turbulent Flow over Convex Surface. AIAA Paper 2002-2828 (2002)
4. Han, G., Zhou, M.D., and Wygnanski, I.: On Streamwise Vortices in a Turbulent Wall Jet Flowing over a Circular Cylinder. AIAA Paper 2004-2350 (2004)
5. Likhachev, O., Neuendorf, R., and Wygnanski, I.: On Streamwise Vortices in a Turbulent Wall Jet that Flows over a Convex Surface. Physics of Fluid, **13(6)**, 1822–1825 (2001)
6. Pajayakrit, P., and Kind, R.J.: Streamwise Vortices in the Outer Layer of Wall Jets with Convex Curvature. AIAA Journal, **37(2)** 281–283 (1999)
7. Wernz, S.H., Valsecchi, P., Gross, A., and Fasel, H.F.: Numerical Investigation of Transitional and Turbulent Wall Jets Over a Convex Surface. AIAA Paper 2003-3727 (2003)
8. Wernz, S.H., Gross, A., and Fasel, H.F.: Numerical Investigation of Coherent Structures in Plane and Curved Wall Jets. AIAA Paper 2005-4911 (2005)
9. Gross, A., Fasel, H.F.: Coanda Wall Jet Calculations Using One- and Two-Equation Turbulence Models. AIAA Journal, **44(9)** 2095–2107 (2006)
10. Swanson, R., Rumsey, C., and Sanders, S.: Progress Towards Computational Method for Circulation Control Airfoils. AIAA Paper 2005-89 (2005)
11. Kulfan, B.M. and Bussoletti J.E.: "Fundamental" Parametric Geometry Representation for Aircraft Component Shapes. AIAA-2006-6948, (2006)
12. Kulfan, B.M.: Universal Parametric Geometry Representation Method. J. of Aircraft. **45(1)**, 142–158 (2008)
13. Kulfan, B.M.: Recent Extensions and Applications of the 'CST' Universal Parametric Geometry Representation Method. RAeS Journal. **45(1)**, 157–176 (2010)
14. http://www.sourceforge.net/projects/caffasst
15. Perić, M., Ferziger, J.: Computational Methods for Fluid Dynamics. Springer, Berlin (2000)
16. Menter, F., et. al.: The SST Turbulence Model with Improved Wall Treatment for Heat Transfer Predictions in Gas Turbines. Proceedings of the International Gas Turbine Congress, Tokyo, November 2-7, 2003.
17. Mirkov, N., Rašuo, B. : Numerical Simulation of Air Jet Attachment to Convex Walls and Applications. Proceedings of 27th International Congress of the Aeronautical Sciences, Nice, France 2010.
18. Mirkov, N., Rašuo, B. : Maneuverability of an UAV with Coanda Effect Based Lift Production. Proceedings of 28th International Congress of the Aeronautical Sciences, Brisbane, Australia 2012.